Anion Binding with Two Polyammonium Macrocycles of Different Dimensionality

Thomas Clifford,[†] Andrew Danby,[†] José M. Llinares,[†] Susan Mason,[†] Nathaniel W. Alcock,[§] Douglas Powell,[†] Juan A. Aguilar,[‡] Enrique García-España,[‡] and Kristin Bowman-James*[,†]

Department of Chemistry, University of Kansas, Lawrence, Kansas 66045, Department of Chemistry, University of Warwick, Coventry CV4 7AL, U.K., and Departamento de Química Inorgánica, Facultad de Química, Universidad de Valencia, c/Dr. Moliner, 50, 46100 Burjassot, Valencia, Spain

Received January 31, 2001

A comparative study of the binding of nitrate and sulfate with a polyammonium monocycle **L**[1], (3,6,9,17,20,23-hexaazatricyclo[23.3.1.1[11,15]]-triaconta-1(29),11,13,15(30),25,27-hexaene), and the corollary bicycle **L**[2], (1,4,12,15,18,26,31,39-octaazapentacyclo-[13.13.13.1[6,10].1[20,24].1[33,37]]-tetratetraconta-6,7,9,20(43),21,23,33-(42),34,36-nonaene), is reported. Potentiometric studies indicated negligible binding for **L**[1] and nitrate, but high affinity was observed for sulfate ($\log K_{H_5L(SO_4)/H_5L\cdot SO_4} = 3.53(1)$, $\log K_{H_6L(SO_4)/H_6L\cdot SO_4} = 4.36(1)$). Stronger binding was observed for the cryptand **L**[2] with both nitrate and sulfate ($\log K_{H_6L(NO_3)/H_6L\cdot NO_3} = 3.11(5)$, $\log K_{H_7L(NO_3)/H_7L\cdot NO_3} = 3.55(5)$; $\log K_{H_6L(SO_4)/H_6L\cdot SO_4} = 4.43(1)$, $\log K_{H_7L(SO_4)/H_7L\cdot SO_4} = 4.97(5)$). Five crystal structures are reported: the nitrate (**1**) and sulfate (**2**) salts of **L**[1], the free base (**3**) of **L**[2], and the nitrate (**4**) and tosylate (**5**) salts of **L**[2]. Structural results for **L**[1] indicate relatively planar monocycles with cis and trans orientations of the phenyl groups for **2** and **1**, respectively, with the anions above and below the monocycle rings. For **L**[2], key features include an encapsulated water and intricate water network in **3**, two encapsulated and four external nitrates and two external water molecules in **4**, and six external tosylates with sulfonate groups pointing into the cavity and eight external waters in **5**.

Introduction

In 1996, we reported crystal structures and molecular dynamics studies of complexes of two protonated mixed aza−oxa macrocycles with nitrate ions ([24]aneN_6O_2 and [18]aneN_4O_2).[1] At that time, few reports of polyammonium complexes with nitrate had been published.[2,3] Nitrate is, however, an anion of increasing focus because of efforts in nuclear waste remediation[4,5] and also because of mounting concern over increased concentrations of nitrate in the groundwaters of agricultural regions.[6−8] The crystal structures of the two complexes were quite different. The structure of the larger 24-membered ring macrocycle showed a single nitrate enfolded in a boatlike cyclic cavity with remaining nitrate counterions associated via hydrogen-bonding interactions outside the cavity. The structure of the smaller macrocycle showed nitrates above and below a relatively planar cyclic cavity. Molecular dynamics studies indicated that in solution, these types of monocycles were prone to flatten[1] or to remain flat[1,9] because of solvation effects, thereby lessening their promise for achieving selective binding of anions in solution.

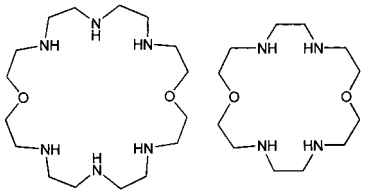

Because of the increasingly widespread interest in anion chemistry,[10−20] we decided to continue our investigations, focusing on the binding of simple anions, and primarily oxo

[†] University of Kansas.
[§] University of Warwick.
[‡] Universidad de Valencia.

(1) Papoyan, G.; Gu, K.; Wiórkiewicz-Kuczera, J.; Kuczera, K.; Bowman-James, K. *J. Am. Chem. Soc.* **1996**, *118*, 1354−1364.
(2) Cullinane, J.; Gelb, R. I.; Margulis, T. N.; Zompa, L. J. *J. Am. Chem. Soc.* **1982**, *104*, 3048−3053.
(3) Cramer, R. E.; Fermin, V.; Kuwabara, E.; Kirkup, R.; Selmna, M.; Akoi, K.; Adeyemo, K. A.; Yamazaki, H. *J. Am. Chem. Soc*. **1991**, *113*, 7033−7034.
(4) *Science and Technology for Disposal of Radioactive Tank Wastes*; Schultz, W. W., Lombardo, N. J., Eds.; Plenum: New York, 1998.
(5) Gephart, R. E.; Lundgren, R. E. *Hanford Tank Cleanup: A Guide to Understanding the Technical Issues*; Report PNL-10773; Pacific Northwest National Laboratory: Richland, Washington, 1995.
(6) Mason, C. F. *Biology of Freshwater Pollution*, 2nd ed.; Longman: New York, 1991.
(7) *Sci. Am.* **1996**, *275*, 24.
(8) Bouchard, D. C.; Williams, M. K.; Surampalli, R. Y. *J. Am. Water Works Assoc*. **1992**, *84*, 85−90.
(9) Wiórkiewicz-Kuczera, J.; Kuczera, K.; Bazzicalupe, C.; Bencini, A.; Valtancoli, B.; Bianchi, A.; Bowman-James, K. *New J. Chem.* **1999**, *23*, 1007−1013.
(10) *Supramolecular Chemistry of Anions*; Bianchi, A., Bowman-James, K., García-España, E., Eds.; Wiley-VCH: New York, 1997.
(11) Beer, P. D.; Smith, D. K. *Prog. Inorg. Chem.* **1997**, *46*, 1−96.
(12) Crompton, T. R. *Determination of Anions*; Springer: New York, 1996.
(13) Dietrich, B. *Pure Appl. Chem.* **1993**, *65*, 1457−1464.
(14) Sessler, J. L.; Cyr, M.; Furuta, H.; Kral, V.; Mody, T.; Morishma, T.; Shionaya, M.; Weghorn, S. *Pure Appl. Chem.* **1993**, *65*, 393−398.
(15) Beer, P. D.; Wheeler, J. W.; Moore, C. In *Supramolecular Chemistry*; Balzani, V., De Cola, L., Eds.; Kluwer Academic Publishers: Dordrecht, Netherlands, 1992; pp 105−118.
(16) Martell, A. E. In *Crown Compounds: Towards Future Applications*; Cooper, S. R., Ed.; VCH Publishers: New York, 1992; Chapter 7, pp 99−131.
(17) Katz, H. E. In *Inclusion Compounds*; Atwood, J. L., Davies, J. E. D., MacNichol, D. D., Eds.; Oxford University Press: Oxford, U.K., 1991; pp 391−405.
(18) Izatt, R. M.; Pawlak, K.; Bradshaw, J. S.; Bruening, R. L. *Chem. Rev.* **1991**, *91*, 1721−2085.
(19) Mertes, M. P.; Mertes, K. B. *Acc. Chem. Res.* **1990**, *23*, 413−418.
(20) Kimura, E. *Top. Curr. Chem.* **1985,** *128,* 113−141.

10.1021/ic010135l CCC: $20.00
Published on Web 07/31/2001

anions, with polyammonium macrocycles. Although these studies commenced with polyammonium monocycles, they soon broadened to include the bicyclic analogues in order to obtain systems with greater rigidity for engulfing and retaining targeted anions. For ease of synthesis, we examined receptors readily obtainable from borohydride reductions of macrocycles derived from Schiff base condensations. The general synthetic methodology for an entire series of reduced Schiff base-derived macrocycles was first reported by Martell and co-workers,[21] and today, a number of researchers worldwide are taking advantage of these easily accessible macrocycles. Nelson and co-workers were the first to demonstrate that multiatomic oxo anions could actually be incorporated inside the macrocyclic cavity of these systems.[22]

Key to targeting selective receptors for anions is the determination of the affinities of any given receptor for a variety of anions. Unfortunately, determining binding constants for anions, not to mention measuring pK_a's for polyamine-based systems using potentiometric pH-metric techniques, is complicated because of the necessity of maintaining a constant ionic strength. In this regard, finding a suitable electrolyte becomes a limiting factor. Interference of the electrolyte anion can influence not only the anion binding constants but also the observed pK_a's, particularly if the electrolyte anion can bind to the receptor.[23−26] Hence, a number of researchers have resorted to electrolytes with bulky anions, such as tosylate and related phenylsulfonate systems, to circumvent binding interference. We have recently employed ^{19}F NMR spectroscopy to explore the solution interaction of fluoride with $\mathbf{L}^2$, and the results indicated that tosylate does not interfere with internal binding (encapsulation) of the small halide.[27] Given these findings, the crystal structure of the hexatosylate salt of $\mathbf{L}^2$ was of interest in order to examine how the bulky anion would influence the shape of the cryptand and whether the terminal sulfonate groups would enter the cavity.

This paper describes a comparative study of the binding of nitrate and sulfate with two macrocycles of different dimensionality derived from isophthalaldehyde: a monocycle, $\mathbf{L}^1$, derived from a Schiff base condensation with dien (diethylenetriamine) and its corollary bicycle, $\mathbf{L}^2$, obtained from a similar condensation with tren (2,2′,2″-aminoethylamine). The resulting receptors are 3,6,9,17,20,23-hexaazatricyclo[23.3.1.1^{11,15}]-triaconta-1(29),11,13,15(30),25,27-hexaene ($\mathbf{L}^1$) and the cryptand 1,4,12,15,18,26,31,39-octaazapentacyclo-[13.13.13.1^{6,10}.1^{20,24}.1^{33,37}]-tetratetraconta-6,7,9,20(43),21,23,33(42),34,36-nonaene ($\mathbf{L}^2$). We previously communicated the unusual occurrence of the ditopic *anion* binding capabilities of $\mathbf{L}^2$ with nitrate,[28] and the structure was also later reported by other workers.[29]

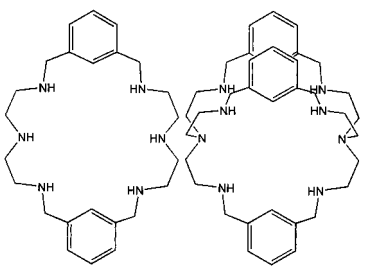

$\mathbf{L}^1$ $\mathbf{L}^2$

1 $[H_6\mathbf{L}^1][NO_3]_6\cdot H_2O$ **3** $\mathbf{L}^2\cdot 12.64H_2O$

2 $[H_6\mathbf{L}^1][SO_4]_3\cdot 5H_2O$ **4** $[H_6\mathbf{L}^2(NO_3)_2][NO_3]_4\cdot 2H_2O$

5 $[H_6\mathbf{L}^2][TsO]_6\cdot 8H_2O$

Experimental Section

Sodium or potassium salts of the anions were purchased as reagent grade and were used without further purification. Sodium *p*-toluenesulfonate (NaTsO), NaOH, and *p*-toluenesulfonic acid (TsOH) were purchased from Aldrich, and the sodium salt was recrystallized from diethyl ether dried under vacuum before use. Potassium *p*-toluenesulfonate (KTsO) was prepared by the neutralization of TsOH with KOH (Fisher) in EtOH/H_2O, followed by recrystallization three times from EtOH/H_2O. Solutions of NaOH (0.1 M) were prepared by dilution of a chilled 10 M solution of high-purity NaOH and standardized by titration of weighed samples of potassium hydrogen phthalate. Standard HCl (0.1006 M) was purchased from Aldrich. Water was triply distilled in an all-glass still.

Synthesis. The ligands $\mathbf{L}^1$ and $\mathbf{L}^2$ were prepared by literature methods[30,31] and were purified by twice recrystallizing as the hydrochloride salt followed by isolation of the free base using ion exchange chromatography (DOWEX 2X8-100, Aldrich). The nitrate and sulfate complexes of $\mathbf{L}^1$ (**1** and **2**, respectively) were prepared by dissolving the free base in methanol and adjusting the pH to 3 by addition of the appropriate acid.[32] The nitrate salt of $\mathbf{L}^2$ (**4**) was prepared by dissolving the free base in CH_3OH and adjusting the pH to 3 by addition of concentrated HNO_3.[33] The tosylate salts of $\mathbf{L}^1$ and $\mathbf{L}^2$ were prepared by adding a CH_3OH solution of the free base to TsOH[34] according to published procedures.[35,36] In each case, the product precipitated after stirring at room temperature or after refrigeration.

$\mathbf{L}^2\cdot x\mathbf{H_2O}$, 3. Crystalline $\mathbf{L}^2$ was prepared by adding an excess of 0.1 M NaOH (0.927 g, 23.2 mmol in 10 mL of H_2O) to a stirring 0.03 M solution of $[H_8\mathbf{L}^2][Cl]_8$ (0.962 g, 1.18 mmol, dissolved in 25 mL of

(21) Chen, D.; Martell, A. E. *Tetrahedron* **1991**, *47*, 6895−6902.

(22) Morgan, G.; McKee, V.; Nelson, J. *J. Chem. Soc., Chem. Commun.* **1995,** 1649−1652.

(23) Motekaitis, R. J.; Martell, A. E.; Lehn, J.-M.; Watanbe, E. I. *Inorg. Chem.* **1982**, *21*, 4253−4257.

(24) Motekaitis, R. J.; Martell, A. E.; Dietrich, B.; Lehn, J.-M. *Inorg. Chem.* **1984**, *23*, 1588−1591.

(25) Motekaitis, R. J.; Martell, A. E.; Murase, I. *Inorg. Chem.* **1986,** *25*, 938−944.

(26) Wu, G.; Izatt, R. M.; Bruening, M. L.; Jiang, W.; Azab, H.; Krakowiak, K. E.; Bradshaw, J. S. *J. Inclusion Phenom. Mol. Recognit. Chem.* **1992**, *13*, 121−127.

(27) Mason, S.; Llinares, J. M.; Morton, M.; Clifford, T.; Bowman-James, K. *J. Am. Chem. Soc.* **2000**, *122*, 1814−1815.

(28) Mason, S.; Clifford, T.; Seib, L.; Kuczera, K.; Bowman-James, K. *J. Am. Chem. Soc.* **1998**, *120*, 8899−8900.

(29) Hynes, M. J.; Mauber, B.; McKee, V.; Town, R. M.; Nelson, J. *J. Chem. Soc., Dalton Trans.* **2000**, 2853−2859.

(30) Nation, D. A.; Martell, A. E.; Carroll, R. I.; Clearfield, A. *Inorg. Chem.* **1996**, *35*, 7246−7252.

(31) Menif, R.; Reibenspies, J.; Martell, A. E. *Inorg. Chem.* **1991**, *30*, 3446−3454.

(32) Anal. Calcd for $[C_{24}H_{44}N_6][NO_3]_6$: C, 36.55; H, 5.62; N, 21.31; O, 36.52. Found: C, 36.48; H, 5.86; N, 21.40; O, 36.19. FAB-MS (H_2O−NBA) *m*/*z*: 411, corresponding to $[M + 1]^+$, 474 $[M + NO_3]^+$, 537 $[M + 2(NO_3)]^+$, 600 $[M + 3(NO_3)]^+$. Anal. Calcd for $[C_{24}H_{44}N_6][SO_4]_3\cdot 3H_2O$: C, 38.02; H, 6.65; N, 11.09; O, 31.67; S, 12.69. Found: C, 36.44; H, 6.51; N, 11.03; O, 28.78; S, 12.49. FAB-MS (H_2O−NBA) *m*/*z*: 411, corresponding to $[M + 1]^+$, 509 $[M + SO_4]^+$, 607 $[M + 2(SO_4)]^+$, 705 $[M + 3(SO_4)]^+$.

(33) Anal. Calcd for $[C_{36}H_{60}N_8(NO_3)_2][NO_3]_4\cdot 2H_2O$: C, 42.68; H, 6.37; N, 19.36. Found: C, 42.72; H, 6.59; N, 19.19. FAB-MS (H_2O−NBA) *m*/*z*: 599, corresponding to $[M + 1]^+$, 662 $[M + NO_3]^+$, 725 $[M + 2(NO_3)]^+$, 788 $[M + 3(NO_3)]^+$, 851 $[M + 4(NO_3)]^+$. ^{1}H NMR (400 MHz, D_2O): 2.72 (t, 12H, N-CH_2), 3.14 (t, 12H, CH_2−NH_2), 4.10 (s, 12H, benz−CH_2), 7.23 (s, 3H, benz), 7.45 (m, 9H, benz). ^{13}C NMR (400 MHz, D_2O): 45.79 (N−CH_2), 50.98 (CH_2−NH_2), 51.81 (benz−CH_2), 130.42 (benz), 131.35 (benz), 131.46 (benz), 131.77 (benz).

(34) Anal. Calcd for $C_{36}H_{54}N_8\cdot 8HTs\cdot 4H_2O$: C, 53.94; H, 6.20; N, 5.47. Found: C, 53.84; H, 6.17; N, 5.71. ^{1}H NMR (400 MHz, D_2O): 2.36 (s, 24H, CH_3), 2.82 (t, 12H, CH_2−N), 3.12 (t, 12H, CH_2−NH_2), 4.11 (s, 12H, benz−CH_2), 7.20 (s, 3H, benz), 7.33 (d, 16H, Ts), 7.44 (m, 9H, benz), 7.63 (d, 16H, Ts). ^{13}C NMR (400 MHz, D_2O): 20.82, 44.93, 50.71, 51.30, 125.65, 129.86, 130.65, 131.30, 131.49, 131.94, 139.72, 142.94.

(35) Dietrich, B.; Lehn, J.-M.; Guilhem, J.; Pascard, C. *Tetrahedron Lett.* **1989**, *30*, 4125−4128.

(36) Dietrich, B.; Dilworth, B.; Lehn, J.-M.; Souchez, J.-P.; Cesario, M.; Guilhem, J.; Pascard, C. *Helv. Chim. Acta* **1996**, *79*, 569−587.

Table 1. Crystallographic Data for $[H_6\mathbf{L}^1][NO_3]_6\cdot H_2O$ (**1**), $[H_6\mathbf{L}^1][SO_4]_3\cdot 5H_2O$ (**2**), $\mathbf{L}^2\cdot 12.64H_2O$ (**3**), $[H_6\mathbf{L}^2(NO_3)_2][NO_3]_4\cdot 2H_2O$ (**4**), and $[H_6\mathbf{L}^2][TsO]_6\cdot 8H_2O$ (**5**)

	1	**2**	**3**	**4**	**5**
empirical formula	$C_{24}H_{46}N_{12}O_{19}$	$C_{24}H_{54}N_6O_{17}S_3$	$C_{36}H_{79.27}N_8O_{12.64}$	$C_{36}H_{64}N_{14}O_{20}$	$C_{78}H_{118}N_8O_{26}S_6$
fw	806.73	749.91	826.50	1013.01	1776.16
cryst syst	monoclinic	orthorhombic	monoclinic	triclinic	triclinic
space group	$P2_1/n$	*Amm*2	*Cc*	$P\bar{1}$	$P\bar{1}$
a (Å)	13.6738(8)	10.7345(3)	10.6236(9)	10.240(2)	13.726(2)
b (Å)	8.2208(5)	29.6422(4)	18.5875(15)	10.369(2)	14.990(3)
c (Å)	15.5074(9)	5.7286(2)	23.978(2)	25.633(2)	22.818(5)
α (deg)	90.00	90.00	90.00	80.46(3)	79.04(2)
β (deg)	94.633(2)	90.00	100.325(2)	84.96(3)	82.05(2)
γ (deg)	90.00	90.00	90.00	62.23(3)	83.39(2)
V (Å^3)	1737.48(18)	1822.81(9)	4658.2(7)	2374.7(8)	4545.9(14)
Z	2	2	4	2	2
diffractometer	Smart CCD	Smart CCD	Smart CCD	AFC5R	AFC5R
d_{calcd} (g/cm^3)	1.542	1.448	1.179	1.417	1.298
λ (Å)	0.710 73	0.710 73	0.710 73	1.541 78	1.541 78
T (K)	173(2)	180(2)	173(2)	296(2)	296(2)
F(000)	852	848	1809	1076	1892
abs coeff (mm^{-1})	0.133	0.283	0.089	0.992	2.033
abs corr	none	multiscan	multiscan	empirical	empirical
max, min transm		0.93, 0.65	0.99, 0.96	0.86, 0.76	0.82, 0.69
θ range (deg)	2.07−28.26	2.75−28.42	2.24−25.50	1.75−57.79	1.99−60.07
reflns collected	11 562	5542	14 205	6986	14 130
indep reflns	3955	2223	7714	6558	13 530
data/restr/params	3955/0/253	2223/37/158	7714/20/542	6558/0/631	13530/210/1068
R1; wR2[a]	0.0509; 0.1479	0.0587; 0.1527	0.0587; 0.1674	0.0521; 0.1442	0.0771; 0.2388
GOF (F^2)	1.033	1.128	1.008	1.056	1.057

[a] R1 (obsd data) $= \sum||F_o| - |F_c||/\sum|F_o|$. wR2 (all data) $= \{\sum[w(F_o^2 - F_c^2)^2]/\sum[w(F_o^2)^2]\}^{1/2}$.

H_2O) at room temperature under atmospheric conditions. Platelike, colorless crystals began to precipitate within 5 min and were filtered, washed with cold water (3 × 5 mL), and dried under vacuum. Yield: 0.536 g, 55%. Anal. Calcd for $C_{36}H_{54}N_8\cdot 9H_2O$: C, 56.82; H, 9.54; N, 14.72. Found: C, 57.00; H, 8.50; N, 14.60. FAB-MS (CH_3OH−NBA) *m*/*z*: 599, corresponding to $[M + 1]^+$. ^{1}H NMR (400 MHz, $CDCl_3$): 7.21 (m, 3H, Ar*H*), 7.16 (s, 3H, Ar*H*), 7.14 (d, 6H, Ar*H*), 3.63 (s, 12H, CH_2−Ar), 2.64 (t, 12H, CH_2NH), 2.57 (t, 12H, CH_2−N). ^{13}C NMR (400 MHz, $CDCl_3$): 141.14, 128.52, 127.63, 127.21, 55.64, 54.12, 48.04.

Potentiometric Methods. The glass electrode was calibrated as a hydrogen ion concentration probe by titration of previously standardized amounts of HCl with CO_2-free NaOH solutions in a water-jacketed cell. The electrode response was checked by plotting the data by Gran's method[37,38] (Na_2CO_3 was estimated to be less than 2% in all titrations), which gives the standard potential ($E°$) and the ionic product of water ($pK_w = 13.73(1)$). The data were treated using the program ESTA2B[39] or PASAT.[40] Titration pH data were then corrected in a spreadsheet (microcal origin) using these parameters before being processed in HYPERQUAD[41,42] or, as previously described,[43] in SUPERQUAD.[44] In a typical data set for an anion complexation experiment, three curves were collected (ca. 100 points each) over a pH range of 2.5−11.0. Ligand concentration (obtained either from titration of the free base with copper(II) or by using a weighed amount of the analyzed tosylate salt) was 1 mM, and anion concentrations were 1, 2, and 3 mM. Inspection of [B]/[L] plots of the titration of H_6L^{6+} compared to H_6L^{6+} in the presence of anion revealed the probable species to be included in the model. All measurements were made at 25.0 °C.

NMR Methods. Binding Constants. A 50 cm^3 solution (10% D_2O in H_2O and 0.3 mL of *t*-BuOH as internal standard) of 2 mM in ligand and 12 mM in KTsO was titrated with the potassium salt of the anion under investigation (50 mM solution), maintaining pH at 3.0 ± 0.05 throughout the experiment. After each aliquot, a sample from the cell was removed and its ^{1}H NMR spectrum was recorded using a presaturation pulse to suppress the HDO signal. All measurements were made at 25.0 °C. The association constants were determined from the binding curves of multiple $-CH_2-$ protons using EQNMR.[45]

X-ray Crystallography. Crystal data and details of the data collection for the anion complexes of $\mathbf{L}^1$ and $\mathbf{L}^2$ are given in Table 1. For **1**, **2**, and **3**, crystal data were collected and integrated using Bruker SMART systems, with graphite monochromated Mo Kα radiation ($\lambda = 0.710\ 73$ Å) at 173−180 K.[46,47] Measurements for **4** and **5** were made at room temperature on a Rigaku AFC5R diffractometer with graphite monochromated Cu Kα radiation ($\lambda = 1.541\ 78$ Å) and a rotating anode generator.[48] The crystals were monitored for decay during data collection, and corrections for decay were made, if warranted. Lorentz and polarization corrections were applied, as well as semiempirical absorption corrections. The structures were solved by direct methods and refined by full-matrix least-squares methods on F^2.[47] Non-hydrogen atoms were refined with anisotropic displacement parameters. The positions of hydrogen atoms bonded to nitrogen atoms were often located from difference Fourier maps; other hydrogen atoms were either located from difference maps or placed at calculated positions. Hydrogen atoms were refined using a riding model with fixed isotropic displacement parameters that were 1.2−1.5 times the equivalent isotropic displacement parameter for the atom to which a given hydrogen atom was bonded. Torsion angles and hydrogen-bonding

(37) Gran, G. *Analyst (London)* **1952**, *77*, 661−671.
(38) Rosotti, F. J. C.; Rossotti, H. *J. Chem. Educ.* **1965**, *42*, 375−378.
(39) May, P. M.; Murray, K.; Williams, D. R. *Talanta* **1988**, *35*, 825−830.
(40) Fontanelli, M.; Micheloni, M. *Proceedings of the I Spanish-Italian Congress on the Thermodynamics of Metal Complexes*; Diputación de Castellón: Castellón, Spain.
(41) Gans, P.; Sabatini, A.; Vacca, A. *Coord. Chem. Rev.* **1992**, *120*, 389−405.
(42) Gans, P.; Sabatini, A.; Vacca, A. *Talanta* **1996**, *43*, 1739.
(43) García-España, E.; Ballester, M.-J.; Lloret, F.; Moratal, J.-M.; Faus, J.; Bianchi, A. *J. Chem. Soc., Dalton Trans.* **1988**, 101−104.
(44) Gans, P.; Sabatini, A.; Vacca, A. *J. Chem. Soc., Dalton Trans.* **1995**, 1195−1200.
(45) Hynes, M. J. *J. Chem. Soc., Dalton Trans.* **1993**, 311−312.
(46) Structure data for **1** and **3** were obtained at the X-ray Crystallography Laboratory at Kansas State University, and structure data for **2** were obtained at the X-ray Crystallography Laboratory at the University of Warwick.
(47) Sheldrick, G. *SHELX-97 Program for Crystal Structure Solution*; Institüt für Anorganische Chemie der Universität: Gottingen, Germany, 1997. Sheldrick, G. *SHELX-97 Program for Crystal Structure Refinement*; Institüt für Anorganische Chemie der Universität: Gottingen, Germany, 1997.
(48) Structures **4**−**6** were obtained at the X-ray Crystallography Laboratory at the University of Kansas using: *MSC/AFC Diffractometer Software*; Molecular Structure Corporation: The Woodlands, TX.

distances for the $\mathbf{L}^1$ complexes are given in Tables 2 and 3, respectively, and for $\mathbf{L}^2$ and its complexes in Tables 4 and 5, respectively.

A. $[H_6L^1][NO_3]_6\cdot H_2O$, 1. Crystals suitable for X-ray analysis were obtained by recrystallization of the nitrate salt from a CH_3OH/H_2O solution (5:1, v/v). The hexacation was found to sit on a crystallographic center of symmetry. The water molecule was located near the center of symmetry and thus was modeled with 50% occupancy.

B. $[H_6L^1][SO_4]_3\cdot 5H_2O$, 2. Crystals suitable for X-ray analysis were obtained by recrystallization of the sulfate salt from a CH_3OH/H_2O solution (5:1, v/v). The cationic species and one water molecule sit on *mm*2 crystallographic sites. The two sulfates sit on crystallographic mirror sites. One of the sulfates, S(2)−O(23), was assigned an occupancy of 0.5 because of its proximity to its symmetry-related self. The other two water molecules were also assigned occupancies of 0.5 because of close contacts with other species. Two hydrogen atoms of O(3), H(3OB) and H(3OC), were assigned relative occupancies of 0.5 of O(3) because they represent contacts to symmetry-related O(3) molecules. Restraints on the displacement parameters of O(21)−O(23) and the water oxygen atoms were required for the refinement to achieve convergence.

C. $L^2\cdot 12.64H_2O$, 3. The crystals obtained from the preparation of the crystalline free base were suitable for X-ray analysis. An attempt to determine the absolute structure by refinement of the Flack parameters,[49] with polar axis restraints taken from Flack and Schwarzenbach,[50] resulted in values which were indeterminant. The crystal structure data indicated one neutral cage molecule and, on average, 12.64 water molecules found per asymmetric unit. A central partial water molecule was actually split over three locations that were physically too close to accommodate more than one water at a time. The occupancies for these water molecules were refined to 0.306(11), 0.181(9), and 0.148(9) for O(1S), O(2S), and O(3S), respectively. The displacement parameters of the water molecules in the center of the cage were constrained to be equal. There were also two other sites of disorder involving O(1W) and O(6W). The occupancies of these two external water sites were also related because the hydrogen-bonded sites of O(1W′) and O(6W′) (as related by symmetry) were too close to allow these H_2O molecules to exist in the same unit cell. The occupancies refined to 0.532(7) for O(1W) and O(6W′) and to 0.468(7) for O(6W) and O(1W′). Restraints on the displacement parameters of five water molecules were required for the refinement to achieve convergence.

D. $[H_6L^2(NO_3)_2][NO_3]_4\cdot 2H_2O$, 4. The octahydrochloride salt of $\mathbf{L}^1$ (0.100 g, 0.123 mmol) was reacted with $AgNO_3$ (0.125 g, 0.736 mmol) in water (5 mL). After filtration of the precipitated AgCl, the solution was stirred an additional 30 min and centrifuged, and water was removed. Crystals suitable for X-ray analysis were obtained by recrystallization of the product from $EtOH/H_2O$ (2 mL:6 drops).

E. $[H_6L^2][TsO]_6\cdot 8H_2O$, 5. Crystals suitable for X-ray analysis were obtained from an aqueous solution of the octatosylate salt, 0.1 M in KTsO, in the presence of NaF (1:1, $\mathbf{L}^2$/F) at pH ca. 3. (The actual goal of the crystallization was to determine if a mixed fluoride/tosylate salt could be obtained with fluoride in the macrocyclic cavity.) The structure results indicated one disordered molecule of water (O(8)), which refined with occupancy factors of 0.682(14) (O(8A)) and 0.318(14) (O(8B)).

Results and Discussion

Synthesis. Identifying routes to polyamine macrocycles and cryptands from simple Schiff base condensations of polyamines with aromatic spacers[21,30,31] has facilitated the study not only of transition metal coordination chemistry but also of anion coordination. Indeed, the two-step synthetic procedure with relatively high overall yields (>60%) makes these systems very appealing. Despite their ease of synthesis, however, these cryptands are unwieldy in the free base form because the isolated products are usually viscous oils. For metal ion chemistry, this does not necessarily present a problem because crystalline polyammonium salts can be obtained by acidification with a variety of acids and these salts can be reacted with targeted metal ions to achieve the metal complexes. However, for researchers interested in anion coordination, the presence of other anions can interfere or compete with binding of the desired anion. Hence, the identification of a path to a crystalline free base is highly desirable.

We have found a simple route to obtain the free base of these azacryptands in crystalline form starting with the hydrochloride salt of $\mathbf{L}^2$. The procedure consists of dissolving the hydrochloride salt in water, followed by addition of excess 1.0 M NaOH. Crystals of the product precipitate within 5 min. and are isolated by filtration and rinsing with a minimum amount of chilled water. The procedure works well with the related hydrobromide salts and also with the halide salts of the pyridine and terephthalaldehyde analogues of $\mathbf{L}^2$ [51] but not for tosylate salts.

Crystal Structures. A. Monocyclic Structures. $[H_6L^1]\cdot 6NO_3\cdot H_2O$, 1, and $[H_6L^1][SO_4]_3\cdot 5H_2O$, 2. The crystal structures of the nitrate and sulfate complexes of $\mathbf{L}^1$ both show the macrocycle to be in its hexaprotonated form. Compound **1** contains $\mathbf{L}^1$, six nitrate ions, and a water of crystallization. Compound **2** has three sulfate dianions in addition to $\mathbf{L}^1$, plus five water molecules of crystallization. While $\mathbf{L}^1$ contains a 24-membered ring as does the previously reported nitrate complex with [24]aneN_6O_2,[1] both the nitrate and sulfate complexes of $\mathbf{L}^1$ differ from the earlier structure in two respects: in degree of protonation (+6 as opposed to +4) and in the relatively flat ligand geometry.

For both structures, the macrocycle crystallizes as a relatively planar ellipsoid with the phenyl rings capping the long axis. In **1**, the two phenyl rings are canted from the plane of the macrocycle at an angle of 116.9(3)° in a trans configuration (Figure 1). In **2,** the rings are canted at an angle of 117.5(3)° but in a cis configuration, and the macrocycle is bisected by two mirror (*mm* symmetry) planes (Figure 2). Otherwise the macrocycles, as anticipated, are approximately the same size. The distance across the shorter axis, N(1)···N(1′), is 4.396(3) Å in **1** and 4.599(3) Å in **2**, while the length of the long axis (C(7)···C(7′)) is 10.019(3) Å in **1** and 9.891(4) Å in **2**. Even the torsion angles observed for the two complexes are quite similar, indicating how essentially alike the two structures are (with the exception of the cis and trans orientations of the *m*-xylyl groups) (Table 2). For both **1** and **2**, the torsion angles are almost trans for the NCCN and CNCC angles and gauche at ±60° for the CNCC and ±90° for NCCC angles.

What is unusual in the sulfate structure, **2**, however, compared to other crystal structures of anionic complexes of these Schiff base-derived receptors is the cis orientation of the rings. Structural findings have been reported by Martell and coworkers for the pyrophosphate and oxalate complexes of the furan analogue of $[H_6L^1]^{6+}$ [52] and more recently for the phosphate complex of the larger analogue of $\mathbf{L}^1$ derived from dipropylenetriamine with a *m*-xylyl spacer.[53] In both of these structures, the phenyl group crystallizes in trans orientations. In this regard, the cis orientation observed in **2** is unusual.

Hydrogen-bonding interactions are important and also amazingly similar in both structures. As can be seen from Table 3 and Figure 1, in $[H_6L^1][6NO_3]\cdot H_2O$, **1**, symmetry-related nitrates

(49) Flack, H. D. *Acta Crystallogr.* **1983**, *A39*, 876−881.
(50) Flack, H. D.; Schwarzenbach, D. *Acta Crystallogr.* **1988**, *A44*, 499−506.
(51) Mason, S. Ph.D. Thesis, University of Kansas, 2000.
(52) Lu, Q.; Motekaitis, R. J.; Reibenspies, J. J.; Martell, A. E. *Inorg. Chem.* **1995**, *34*, 4958−4964.
(53) Anda, C.; Llobet, A.; Salvado, V.; Reibenspies, J.; Motekaitis, R. J.; Martell, A. E. *Inorg. Chem.* **2000**, *39*, 2986−2999.

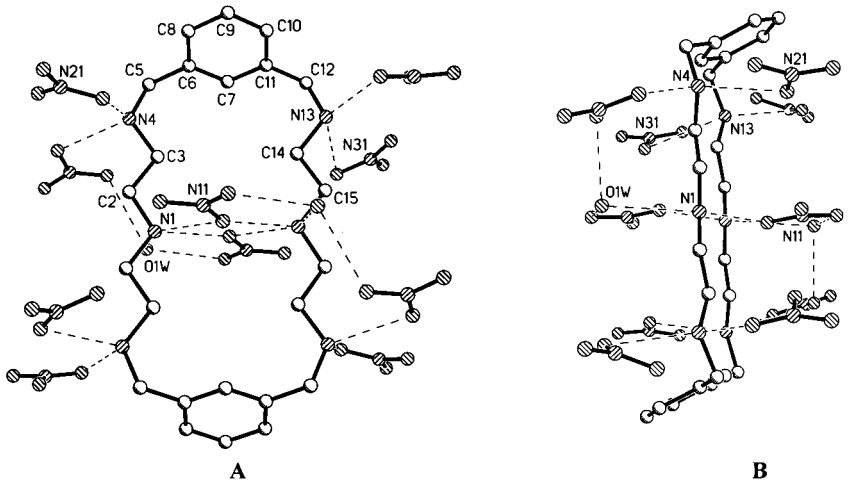

A **B**

Figure 1. Overhead (A) and side (B) views of $[H_6\mathbf{L}^1][NO_3]_6 \cdot H_2O$, **1**, showing the numbering scheme.

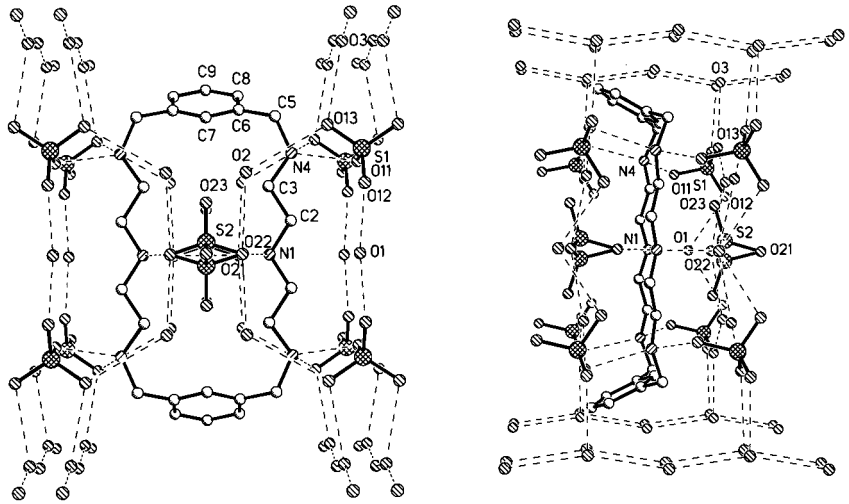

A **B**

Figure 2. Overhead (A) and side (B) views of $[H_6\mathbf{L}^1][SO_4]_3 \cdot 2CH_3OH \cdot H_2O$, **2**, showing the numbering scheme.

Table 2. Selected Torsion Angles (deg) for the $\mathbf{L}^1$ Structures, $[H_6\mathbf{L}^1][NO_3]_6 \cdot H_2O$ (**1**) and $[H_6\mathbf{L}^1][SO_4]_3 \cdot 5H_2O$ (**2**)

atoms	**1**	atoms	**2**
C(15)[a]−N(1)−C(2)−C(3)	−174.40(17)	C(2)[b]−N(1)−C(2)−C(3)	179.9(3)
N(1)−C(2)−C(3)−N(4)	−177.30(15)	N(1)−C(2)−C(3)−N(4)	175.3(4)
C(2)−C(3)−N(4)−C(5)	−169.60(16)	C(2)−C(3)−N(4)−C(5)	−171.1(4)
C(3)−N(4)−C(5)−C(6)	−60.0(2)	C(3)−N(4)−C(5)−C(6)	−60.6(5)
N(4)−C(5)−C(6)−C(7)	95.6(2)	N(4)−C(5)−C(6)−C(7)	97.9(4)
N(4)−C(5)−C(6)−C(8)	−85.2(2)	N(4)−C(5)−C(6)−C(8)	−84.1(4)
C(8)−C(6)−C(7)−C(11)	0.5(3)	C(8)−C(6)−C(7)−C(6)[c]	−0.5(6)
C(5)−C(6)−C(7)−C(11)	179.73(18)	C(5)−C(6)−C(7)−C(6)[c]	−177.6(3)
C(7)−C(6)−C(8)−C(9)	−0.4(3)	C(7)−C(6)−C(8)−C(9)	−0.5(6)
C(5)−C(6)−C(8)−C(9)	−179.58(19)	C(5)−C(6)−C(8)−C(9)	−178.5(3)
C(6)−C(8)−C(9)−C(10)	−0.3(3)	C(6)−C(8)−C(9)−C(8)[c]	1.5(6)
C(8)−C(9)−C(10)−C(11)	0.8(3)	C(8)−C(9)−C(8)[c]−C(6)[c]	−1.5(6)
C(6)−C(7)−C(11)−C(10)	0.0(3)	C(6)−C(7)−C(6)[c]−C(8)[c]	0.5(6)
C(6)−C(7)−C(11)−C(12)	−179.41(18)	C(6)−C(7)−C(6)[c]−C(5)[c]	−177.6(3)
C(9)−C(10)−C(11)−C(7)	−0.6(3)	C(9)−C(8)[c]−C(6)[c]−C(7)	0.5(6)
C(9)−C(10)−C(11)−C(12)	178.75(19)	C(9)−C(8)[c]−C(6)[c]−C(5)[c]	178.5(3)
C(7)−C(11)−C(12)−N(13)	−95.6(2)	C(7)−C(6)[c]−C(5)[c]−N(4)[c]	−97.9(4)
C(10)−C(11)−C(12)−N(13)	85.0(2)	C(8)[c]−C(6)[c]−C(5)[c]−N(4)[c]	82.1(4)
C(11)−C(12)−N(13)−C(14)	56.4(2)	C(6)[c]−C(5)[c]−N(4)[c]−C(3)[c]	60.6(5)
C(12)−N(13)−C(14)−C(15)	165.00(17)	C(5)[c]−N(4)[c]−C(3)[c]−C(2)[c]	171.1(4)
N(13)−C(14)−C(15)−N(1)[a]	168.69(17)	N(4)[c]−C(3)[c]−C(2)[c]−N(1)[d]	−175.3(4)

[a] Symmetry transformations used to generate equivalent atoms for **1**: $-x+1, -y+1, -z+1$. [b] Symmetry transformations used to generate equivalent atoms for **2:** $x, -y+1, z$. [c] Symmetry transformations used to generate equivalent atoms for **2**: $-x+1, y, z$. [d] Symmetry transformations used to generate equivalent atoms for **2**: $-x+1, -y+1, z$.

$(N(11)O_3)$ reside just above and below the two symmetry-related central amines (N(1)). O(13) and its symmetry counterpart dip down toward the cavity and display bifurcated hydrogen bonds with the two central amines at 2.829(2) and 2.779(2) Å. These interactions serve to pull the two aliphatic triamine "sides" of the macrocycle together. N(1) also is linked to the disordered

Table 3. Hydrogen-Bonding Interactions for the $\mathbf{L}^1$ Structures, $[H_6\mathbf{L}^1][NO_3]_6 \cdot H_2O$ (**1**) and $[H_6\mathbf{L}^1][SO_4]_3 \cdot 5H_2O$ (**2**)

1

atoms	distance (Å)	atoms	distance (Å)	atoms	distance (Å)
N(1)−H(1A)···O(13)[a]	2.829(2)	N(4)−H(4A)···O(22)	2.782(2)	N(13)−H(13B)···O(33)[d]	2.897(2)
N(1)−H(1A)···O(1w)	2.926(6)	N(4)−H(4B)···O(22)[c]	2.793(2)	O(1w)−H(1wA)···O(23)[c]	2.847(6)
N(1)−H(1A)···O(1w)[b]	2.977(6)	N(4)−H(4B)···O(23)[c]	3.148(2)	O(1w)−H(1wB)···O(11)[a]	2.708(6)
N(1)−H(1B)···O(13)	2.779(2)	N(13)−H(13A)···O(32)	2.889(3)	O(1w)−H(1wB)···O(13)[a]	2.988(6)
N(1)−H(1B)···O(12)	3.048(2)	N(13)−H(13A)···O(31)	3.062(3)		

2

atoms	distance (Å)	atoms	distance (Å)	atoms	distance (Å)
N(1)−H(11)···O(21)[e]	2.681(6)	N(4)−H(42)···O(11)	2.720(4)	O(2)−H(20B)···O(22)	2.826(16)
N(1)−H(12)···O(22)	2.712(8)	O(1)−H(10A)···O(12)	2.824(7)	O(3)−H(30A)···O(13)	2.866(8)
N(4)−H(41)···O(13)[e]	2.787(5)	O(2)−H(20A)···O(13)	3.211(16)	O(3)−H(30B)···O(3)[f]	2.901(2)
				O(3)−H(30B)···O(3)[g]	2.901(2)

[a] Symmetry transformations used to generate equivalent atoms: $-x+1, -y+1, -z+1$. [b] Symmetry transformations used to generate equivalent atoms: $-x+1, -y+2, -z+1$. [c] Symmetry transformations used to generate equivalent atoms: $-x+{}^1/_2, -y+{}^1/_2, -z+{}^1/_2$. [d] Symmetry transformations used to generate equivalent atoms: $-x+{}^1/_2, y-{}^1/_2, -z+{}^3/_2$. [e] Symmetry transformations used to generate equivalent atoms: $x, y, z-1$. [f] Symmetry transformations used to generate equivalent atoms: $x, -y+{}^1/_2, z-1$. [g] Symmetry transformations used to generate equivalent atoms: $x, -y+{}^1/_2, z+{}^1/_2$.

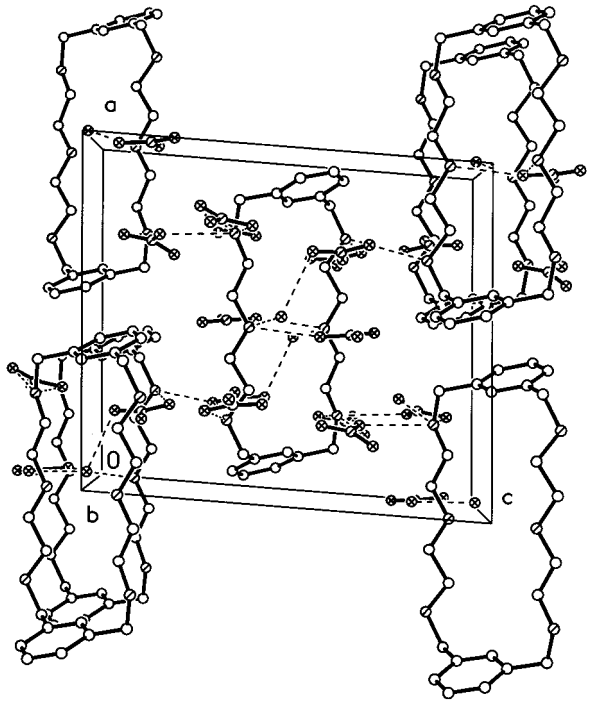

Figure 3. Packing diagram of $[H_6\mathbf{L}^1][NO_3]_6 \cdot H_2O$, **1**, as viewed down the *b* axis. The anions are shown only in the central corridor for clarity.

water molecule as well as more distantly to O(12) of the N(11) nitrate. The other two symmetry-independent amines, N(4) and N(13), are also hydrogen bonded to symmetry-related nitrates above and below the macrocycle: N(4) to O(22) and N(13) to O(32) and their counterparts. The trans orientation of the phenyl rings in **1** appears to be facilitated by the packing as shown in Figure 3. The phenyl rings of adjacent molecules along the *a* axis form loose π-stacking interactions at a distance of 3.405-(3) Å.

In comparison, the similarity in the hydrogen-bonding interactions and placement of the sulfates in **2** may indicate a general trend in oxo anion binding in these simple macrocycles. In $[H_6\mathbf{L}^1][SO_4]_3 \cdot 5H_2O$, **2**, the sulfate directly above the center of the macrocycle exhibits 0.5 occupancy with its disordered counterpart ($S(2)O_4$). This sulfate maintains strong hydrogen bonds to both central ammonium nitrogens, N(1) and its counterpart, via O(22) and its symmetry partner, respectively, (2.705(7) Å) (Figure 2). The 0.5 occupancy of this sulfate is

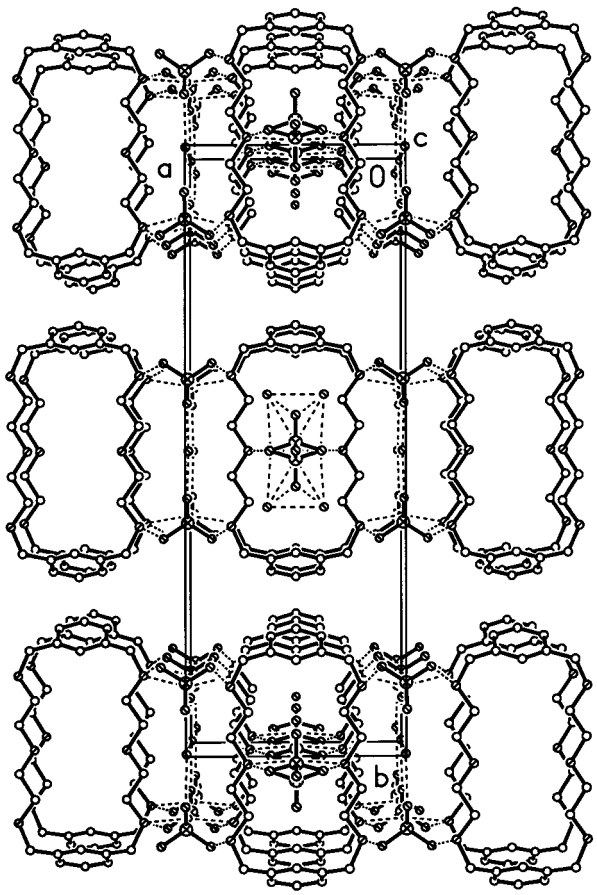

Figure 4. Packing diagram of $[H_6\mathbf{L}^1][SO_4]_3 \cdot 2CH_3OH \cdot H_2O$, **2**, as viewed down the *c* axis. The anions are shown only in the central corridor for clarity.

complicated by the requirements of the space group symmetry. Both disordered sulfates are shown in the figure. The "apical" oxygen of the neighboring symmetry-related sulfate and its disordered counterpart dip into the cavity with even stronger symmetrical bifurcated hydrogen bonds than those in the nitrate structure (vide supra) linking to the two central amines at a distance of 2.686(5) Å. These bridging interactions are largely responsible for stabilizing the elongated macrocycle, as in **1**. The other amines (N(4)) are hydrogen bonded to the remaining sulfates via O(11) and O(13) of S(1) and its three symmetry-

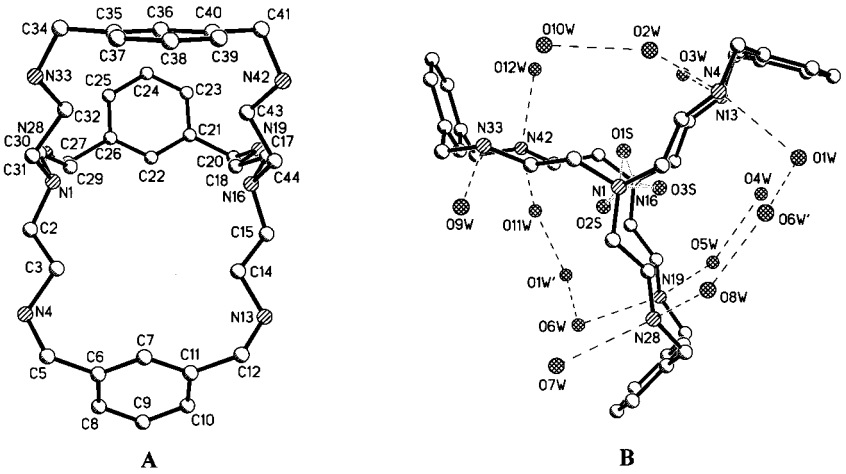

Figure 5. Overhead (A) and side (B) views of $\mathbf{L}^2 \cdot 12.64H_2O$, **3**, showing the numbering scheme. In part A, the water molecules are not shown for a clear view of the cavity.

Table 4. Selected Torsion Angles (deg) for $\mathbf{L}^2 \cdot 12.64H_2O$ (**3**), $[H_6\mathbf{L}^2(NO_3)_2][NO_3]_4 \cdot 2H_2O$ (**4**), and $[H_6\mathbf{L}^2][TsO]_6 \cdot 8H_2O$ (**5**)

atoms	3	4	5
N(1)−C(2)−C(3)−N(4)	167.6(3)	79.9(3)	162.3(5)
N(1)−C(31)−C(32)−N(33)	167.3(3)	82.1(3)	162.3(5)
N(28)−C(28)−C(30)−N(1)	159.5(3)	83.6(3)	−61.3(7)
N(13)−C(14)−C(15)−N(16)	−164.2(4)	−81.4(3)	−172.4(5)
N(16)−C(17)−C(18)−N(19)	−165.7(3)	−85.5(3)	177.0(5)
N(42)−C(43)−C(44)−N(16)	−159.8(3)	−82.7(3)	154.7(6)
N(4)−C(5)−C(6)−C(7)	96.1(4)	−114.3(3)	128.7(6)
N(4)−C(5)−C(6)−C(8)	−82.6(4)	67.8(4)	−54.7(8)
C(10)−C(11)−C(12)−N(13)	77.6(5)	−69.3(4)	71.3(8)
C(7)−C(11)−C(12)−N(13)	−103.6(5)	110.7(3)	−112.2(7)
N(19)−C(20)−C(21)−C(22)	−96.1(4)	107.5(3)	−101.1(7)
N(19)−C(20)−C(21)−C(23)	84.9(4)	−75.7(4)	78.8(7)
C(22)−C(26)−C(27)−N(28)	100.5(9)	−107.3(3)	108.0(7)
C(25)−C(26)−C(27)−N(28)	−80.5(5)	75.4(4)	−72.2(8)
N(33)−C(34)−C(35)−C(36)	95.8(5)	−102.7(4)	−83.3(8)
N(33)−C(34)−C(35)−C(37)	−85.5(5)	80.3(4)	98.1(7)
C(36)−C(40)−C(41)−N(42)	−96.7(5)	109.2(3)	86.5(7)
C(39)−C(40)−C(41)−N(42)	83.1(5)	−73.6(4)	−89.3(7)

related counterparts. These latter interactions are also very similar to those observed in the nitrate complex. Hence, the entire packing scheme consists of a scaffolding network of hydrogen bonds linking layers of macrocycles (Figure 4).

B. Azacryptand Structures. 1. $[\mathbf{L}^2] \cdot 12H_2O$, 3. The complex crystallizes with a complement of water molecules surrounding the macrocycle, comprising an intricate water network as can be seen from Figures 5 and 6. While originally it was thought that the cavity was empty, residual electron density indicated a disordered water molecule symmetrically placed between the arms of the 3-fold apical axis (Figure 5B). Of all of the bicycles, the free base **3** is the most symmetrical in the elegant pinwheel pattern of its *m*-xylyl arms, with almost perfect C_{3h} symmetry. The NCCN angles for each side are approximately trans and almost equal but opposite in sign, ranging from +159.5(3)° to +167.6(3)° for the N(1)CCN sequence and from −159.8(3)° to −165.7° for the N(16)CCN counterparts (Table 4).

The free base structure contains an extensive array of hydrogen-bonded water molecules which lie in the channels between the bicycles along the *c* axis (Figure 6). Four of the secondary amines are linked to these external water molecules via NH···O interactions (Table 5) at about 2.90 Å, while all six of these amines maintain OH···N linkages ranging from 2.8 to 3.04 Å. The disordered internal water molecules are within hydrogen-bonding distances of the two endo lone pairs of the tertiary amines N(1) and N(16), with distances ranging from 2.82(3) to 2.90(3) Å. The internal water molecule is therefore

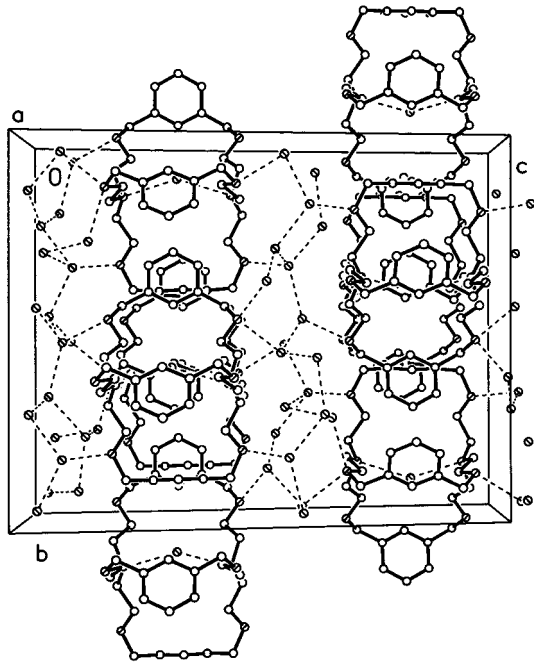

Figure 6. Packing diagram of $\mathbf{L}^2 \cdot 12.64H_2O$, **3**, as viewed down the *a* axis.

clearly the driving force manipulating the shape of the cryptand by pulling the two bridgehead amines inward to a relatively short distance of 5.392(6) Å.

This structure now joins the ranks of only a few examples of structural characterizations of neutral azacryptands. The first was the tiny octaazacryptand structure reported by Smith and co-workers.[54] Nelson and co-workers recently communicated a different structure of $\mathbf{L}^2$ in its free base form, as well as the structure of the related furan analogue.[55] Interestingly, in this other $\mathbf{L}^2$ structure, the free base was crystallized from a hexane/Et_2O mixture and contains no water network or internal water. In the absence of the internal water molecule pulling the bridgehead amines inward, the distance between the these two amines was elongated (10.95 Å). On the other hand, the crystal structure of the furan analogue, while lacking an external water

(54) Smith, P. H.; Barr, M. E.; Brainard, J. R.; Ford, D. K.; Freiser, H.; Muralidharan, S.; Reilly, S. D.; Ryan, R. R.; Silks, L. A.; Yu, W.-H. *J. Org. Chem.* **1993**, *58*, 7939−7941.

(55) Arnaud-Neu, F.; Fuangswasdi, S.; Maubert, B.; Nelson, J.; McKee, V. *Inorg. Chem.* **2000**, *39*, 573−579.

Table 5. Hydrogen-Bonding Distances for $\mathbf{L}^2$ Structures, $\mathbf{L}^2 \cdot 12.64H_2O$ (**3**), $[H_6\mathbf{L}^2(NO_3)_2][NO_3]_4 \cdot 2H_2O$ (**4**), and $[H_6\mathbf{L}^2][Ts]_6 \cdot 8H_2O$ (**5**)

3

atoms	distance (Å)	atoms	distance (Å)	atoms	distance (Å)
N(4)−H(4)···O(2W)	2.911(4)	O(1W′)−H(1WD)···O(11W)	2.613(12)	O(7W)−H(7WA)···N(28)	3.040(8)
N(19)−H(19)···O(6W)	2.893(8)	O(2W)−H(2WA)···O(3W)[b]	2.765(4)	O(7W)−H(7WB)···O(1W)[g]	2.444(10)
N(28)−H(28)···O(8W)	2.903(5)	O(2W)−H(2WB)···O(10W)	2.832(5)	O(8W)−H(8WA)···O(3W)[h]	2.763(5)
N(42)−H(42)···O(12W)	2.903(7)	O(3W)−H(3WA)···N(13)	2.797(5)	O(8W)−H(8WB)···O(4W)[h]	2.827(5)
O(1S)−H(1SA)···N(1)	2.878(15)	O(3W)−H(3WB)···O(9W)[c]	2.713(4)	O(9W)−H(9WA)···N(33)	2.798(5)
O(1S)−H(1SB)···N(16)	2.846(15)	O(4W)−H(4WA)···O(12W)[d]	2.793(5)	O(9W)−H(9WB)···O(5W)[h]	2.741(4)
O(2S)−H(2SA)···N(1)	2.90(3)	O(4W)−H(4WB)···O(5W)	2.830(5)	O(10W)−H(10D)···O(7W)[i]	2.763(5)
O(3S)−H(3SA)···N(1)	2.89(3)	O(5W)−H(5WA)···N(19)	2.901(5)	O(10W)−H(10E)···O(11W)[b]	2.818(5)
O(2S)−H(2SB)···N(16)	2.82(3)	O(5W)−H(5WB)···O(7W)[e]	2.798(6)	O(11W)−H(11D)···N(42)	2.940(5)
O(1W)−H(1WA)···N(4)	2.813(8)	O(6W)−H(6WA)···O(1W′)	2.815(12)	O(11W)−H(11E)···O(9W)[j]	2.768(5)
O(1W)−H(1WB)···O(6W′)	2.794(13)	O(6W′)−H(6WC)···O(8W)	2.740(11)	O(12W)−H(12D)···O(2W)[j]	2.793(5)
O(1W′)−H(1WC)···O(8W)[a]	3.048(11)	O(6W′)−H(6WD)···O(11W)[f]	3.058(11)	O(12W)−H(12E)···O(6W)[i]	2.484(5)
O(1W′)−H(1WD)···O(11W)	2.613(12)				

4

atoms	distance (Å)	atoms	distance (Å)	atoms	distance (Å)
N(4)−H(4A)···O(11)	2.900(4)	N(19)−H(19B)···O(21)	2.979(4)	N(42)−H(42A)···O(22)	3.033(4)
N(4)−H(4A)···O(13)	3.029(4)	N(19)−H(19B)···O(22)	2.923(4)	N(42)−H(42A)···O(23)	2.880(3)
N(4)−H(4B)···O(1W)	2.741(4)	N(28)−H(28A)···O(51)	2.842(3)	N(42)−H(42B)···O(2W)	2.687(4)
N(13)−H(13A)···O(31)	2.847(4)	N(28)−H(28B)···O(11)	2.957(3)	O(1W)−H(1W1)···O(52)[m]	2.827(5)
N(13)−H(13A)···O(33)	3.175(4)	N(28)−H(28B)···O(12)	2.898(4)	O(1W)−H(1W2)···O(1W)[n]	3.008(8)
N(13)−H(13B)···O(21)	2.851(3)	N(33)−H(33A)···O(12)	3.014(4)	O(2W)−H(2W1)···O(31)[o]	3.203(4)
N(13)−H(13B)···O(23)	3.000(3)	N(33)−H(33A)···O(13)	2.874(4)	O(2W)−H(2W2)···O(41)[p]	3.224(4)
N(19)−H(19A)···O(32)[k]	2.888(4)	N(33)−H(33B)···O(52)[l]	2.866(4)	O(2W)−H(2W2)···O(43)[p]	2.953(5)
N(19)−H(19B)···O(21)	2.979(4)				

5

atoms	distance (Å)	atoms	distance (Å)	atoms	distance (Å)
N(4)−H(4B)···O(33)	2.725(8)	N(42)−H(42A)···O(8B)	2.80(2)	O(5)−H(5OB)···O(63)[u]	3.016
N(4)−H(4A)···O(31)[q]	2.778(7)	N(42)−H(42B)···O(42)	2.738(7)	O(6)−H(6OA)···O(3)	2.702(9)
N(13)−H(13A)···O(11)	2.744(6)	O(1)−H(1OA)···O(22)	2.872(8)	O(6)−H(6OB)···O(32)[v]	2.760(10)
N(13)−H(13B)···O(3)	2.831(7)	O(1)−H(1OB)···O(41)	3.118(8)	O(7)−H(7OA)···O(12)[s]	3.512(10))
N(19)−H(19A)···O(2)[#2]	2.747(7)	O(2)−H(2OA)···O(53)	3.041(9)	O(7)−H(7OB)···O(62)	2.942(12)
N(19)−H(19B)···O(52)	2.758(8)	O(2)−H(2OB)···O(63)[t]	2.860(8)	O(8)−H(8OA)···O(13)	2.775(11)
N(28)−H(28A)···O(61)	2.855(7)	O(3)−H(3OA)···O(5)	2.746(8)	O(8)−H(8OB)···O(51)[w]	2.865(10)
N(28)−H(28B)···O(1)	2.869(7)	O(4)−H(4OA)···O(23)[r]	2.741(8)	O(8B)−H(8OC)···O(8B)[w]	2.62(5)
N(33)−H(33A)···O(43)	2.718(8)	O(4)−H(4OB)···O(53)	2.930(9)	O(8B)−H(8OD)···O(51)[w]	2.875(19)
N(33)−H(33B)···O(12)[r]	2.834(7)	O(5)−H(5OA)···O(4)[r]	2.741(8)		
N(42)−H(42A)···O(8A)	2.823(10)				

[a] Symmetry transformations used to generate equivalent atoms: $x - {}^1/_2, -y + {}^3/_2, z + {}^1/_2$. [b] Symmetry transformations used to generate equivalent atoms: $x, -y + 1, z - {}^1/_2$. [c] Symmetry transformations used to generate equivalent atoms: $x + 1, -y + 1, z + {}^1/_2$. [d] Symmetry transformations used to generate equivalent atoms: $x + {}^1/_2, y + {}^1/_2, z$. [e] Symmetry transformations used to generate equivalent atoms: $x + {}^1/_2, -y + {}^3/_2, z + {}^1/_2$. [f] Symmetry transformations used to generate equivalent atoms: $x + {}^1/_2, -y + {}^3/_2, z - {}^1/_2$. [g] Symmetry transformations used to generate equivalent atoms: $x - 1, y, z$. [h] Symmetry transformations used to generate equivalent atoms: $x - {}^1/_2, -y + {}^3/_2, x - {}^1/_2$. [i] Symmetry transformations used to generate equivalent atoms: $x + {}^1/_2, y - {}^1/_2, z$. [j] Symmetry transformations used to generate equivalent atoms: $x, -y + 1, z + {}^1/_2$. [k] Symmetry transformations used to generate equivalent atoms: $x - 1, y, z$. [l] Symmetry transformations used to generate equivalent atoms: $x, y + 1, z$. [m] Symmetry transformations used to generate equivalent atoms: $x + 1, y, z$. [n] Symmetry transformations used to generate equivalent atoms: $-x + 2, -y + 1, -z$. [o] Symmetry transformations used to generate equivalent atoms: $x - 1, y + 1, z$. [p] Symmetry transformations used to generate equivalent atoms: $-x + 1, -y + 1, -z + 1$. [q] Symmetry transformations used to generate equivalent atoms: $-x + 2, -y + 1, -z + 1$. [r] Symmetry transformations used to generate equivalent atoms: $-x + 1, -y + 2, -z$. [s] Symmetry transformations used to generate equivalent atoms: $x + 1, y, z$. [t] Symmetry transformations used to generate equivalent atoms: $-x + 2, -y + 2, -z$. [u] Symmetry transformations used to generate equivalent atoms: $x - 1, y, z$. [v] Symmetry transformations used to generate equivalent atoms: $-x + 1, -y + 1, -z + 1$. [w] Symmetry transformations used to generate equivalent atoms: $-x + 1, -y + 1, -z$.

network, does show a similar disordered internal water molecule and consequently a short distance between the apical amines (5.407 Å).[55]

2. $[H_6L^2(NO_3)_2][NO_3]_4 \cdot 2H_2O$, 4. As noted previously,[28] the trigonally shaped macrocycle is a perfect host for binding the two nitrates, which are held internally by bifurcated hydrogen bonds of the protonated amines (Table 5). Each oxygen atom of the two internal nitrates forms one short (ca. 2.90 Å) and one longer (ca. 3.0 Å) hydrogen bond with two ammonium groups in adjacent arms. Outside of the macrocyclic cavity, four external nitrates and two molecules of water (Figure 7) surround the complex. The symmetrically patterned pinwheel shape is similar to that observed in the structure of the free base **3**. In fact, **4** is a close second to the free base with respect to the highly symmetrical pattern of its structure, as can be seen in its torsion angles which are very comparable to those of **3** (Table 4).

Again, the external water molecules and three of the four nitrates are linked via hydrogen-bonding interactions with the macrocycle. Each of the macrocyclic ammonium groups has one remaining hydrogen atom (after bonding with the two internal nitrates) to participate in hydrogen bonding. N(4) and N(42) display relatively strong hydrogen bonds to O(1W) and O(2W) at 2.741(4) and 2.687(4) Å, respectively. The remaining ammonium groups hydrogen bond with three of the external nitrates (N(13) with O(31); N(28) with O(51); N(19) with a symmetry-related O(32); and N(33) with a symmetry-related O(43)). It is only nitrate N(61) that shows no interactions with

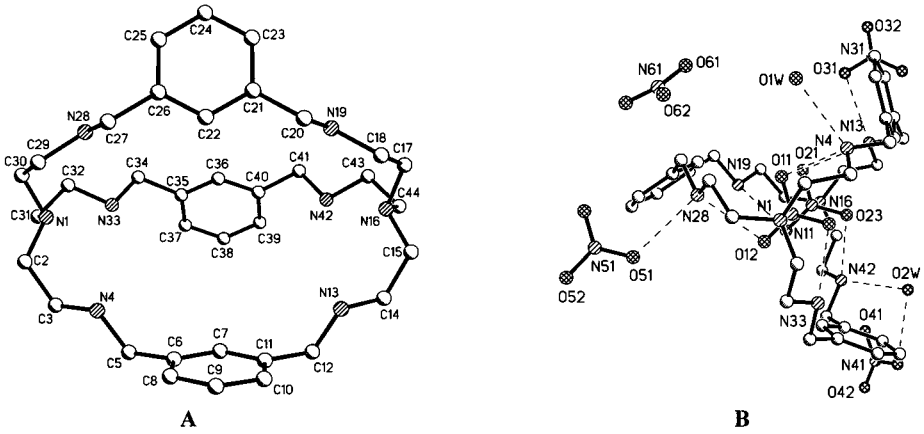

Figure 7. Overhead (A) and side (B) views of $[H_6\mathbf{L}^2(NO_3)_2][NO_3]_4 \cdot 2H_2O$, **4**. In part A, the water molecules and nitrates are not shown for a clear view of the cavity.

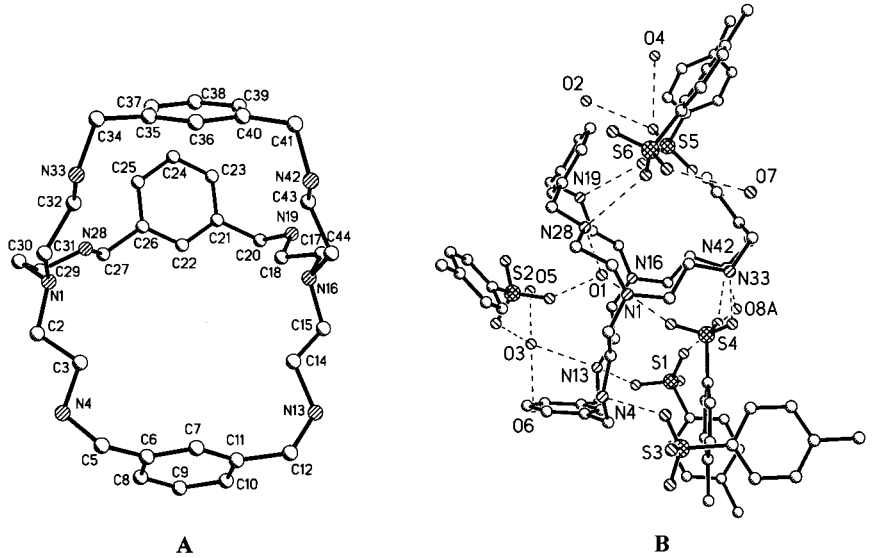

Figure 8. Overhead (A) and side (B) views of $[H_6\mathbf{L}^2][TsO]_6$, **5**. In part A, the water molecules and tosylates are not shown for a clear view of the cavity.

the macrocycle or with surrounding water molecules but appears to be just trapped in the lattice network.

A comparison of the structure of the perchlorate complex of $\mathbf{L}^2$ [29] versus that of the nitrate lends insight to complementarity issues in these systems. In the former structure, perchlorate is also contained inside the $\mathbf{L}^2$ cavity and the tetrahedral oxo anion is oriented with three of its oxygens hydrogen bonded with the three trigonally situated ammonium groups of one tren unit. Three well-placed water molecules additionally serve as bridges to link these oxygens via a hydrogen-bonding network to the ammonium ions of the opposite tren unit. The fourth "axial" oxygen is pointed toward the bridgehead amine of this tren unit, but while it is exceedingly close to the amine (2.559 Å), there is no apparent hydrogen bonding. The hydrogen-bonding pattern of the oxygen atoms tends to break the symmetry of the cryptand and to open one side by spreading the ammonium sites apart, resulting in what the authors call an "Easter egg shape".[29] Thus, the trigonal arrangement of $\mathbf{L}^2$ serves also for binding tetrahedral species but via a very different mode of interaction.

3. $[H_6\mathbf{L}^2][TsO]_6 \cdot 8H_2O$, 5. This complex crystallizes as the hexatosylate salt with eight water molecules of crystallization, including several disordered water molecules with partial occupancies. The C_3 rotation and symmetrical pinwheel-like shape seen for the free base, **3**, and the nitrate complex, **4**, are broken in the structure of **5**. The tosylate ions surround the macrocycle, with each of the sulfonate groups associated with one of the macrocyclic amines (Figure 8, Table 5) with the exception of sulfonate S(2), which is only linked with water molecules in the lattice. As seen in Figure 8A, a view of the macrocycle without the obstructing tosylate groups, the macrocyclic cavity is relatively open with an N(1)···N(16) distance of 7.213(7) Å. Only one of the tosyl groups, S(4), binds across one of the arms (N(33)···N(42)).

Table 6. Stability Constants, log *K*, for the Formation of Sulfate and Nitrate Complexes with $\mathbf{L}^1$ and $\mathbf{L}^2$ Determined in 0.1 mol dm^{-3} NaTsO at 298.1 K

	NO_3^-		SO_4^{2-}	
reaction[a]	$\mathbf{L}^1$	$\mathbf{L}^{2\,b,c}$	$\mathbf{L}^{1\,b,c}$	$\mathbf{L}^{2\,b}$
$H_5L + A = H_5L(A)$			3.53(1) [3.04(2)[d]]	
$H_6L + A = H_6L(A)$		3.11(5)	4.36(1) [4.07(2)[d]]	4.43(1)
$H_7L + A = H_7L(A)$		3.55(5) [3.69]		4.97(5)

[a] Charges omitted for clarity. [b] Values in parentheses are standard deviations in the last significant figure. [c] Brackets indicate NMR data. [d] Data obtained in 0.1 mol dm^{-3} NaCl.

Binding Studies. Binding constants for nitrate and sulfate with $\mathbf{L}^1$ and $\mathbf{L}^2$ were determined and are given in Table 6. The protonation constants for $\mathbf{L}^1$ and $\mathbf{L}^2$ have been determined previously by us[56] and others.[29,31,57,58] While other reports usually include values for the six secondary amines, we

identified a value for the protonation of the seventh, tertiary amine in both this and other[56] work. This finding is not unprecedented as crystal structure data indicate that both seven-[51] and eight-protonated species can exist.[31] In general, however, protonation constants for these systems do tend to vary significantly depending on the experimental conditions employed, being especially sensitive to the electrolyte used to keep the ionic strength constant. For this study, NaTsO was chosen to maintain ionic strength, under the assumption that the bulky tosylate anion would not interact appreciably with the positively charged receptors. Indeed, experiments performed for the interaction of sulfate with $\mathbf{L}^1$ in 0.1 mol dm^{-3} NaCl show slightly lower binding constants ($\log K_{H_6L(SO_4)/H_6L\cdot SO_4} = 4.07(2)$, $\log K_{H_5L(SO_4)/H_5L\cdot SO_4} = 3.04(2)$) than those obtained with NaTsO, potentially indicating interference by chloride (Table 6). Nevertheless, care must be taken in the analysis of the data, and when possible, the use of a technique like NMR is highly recommended in systems characterized by relatively low binding constants (10^2-10^4). With the exception of nitrate binding with $\mathbf{L}^2$, however, the ranges observed for the binding constants were outside of NMR limits and unfortunately precluded the use of NMR for comparative purposes.

An analysis of the data shows that binding of nitrate with $\mathbf{L}^1$ was virtually negligible ($\log K < 2$), in agreement with findings for nitrate binding in a related 24-membered polyammonium macrocycle, [24]aneN$_8$.[9] This finding was anticipated as monovalent ions in general tend to display weaker binding with monocycles as opposed to bicycles. A related study involving fluoride indicated only slightly higher binding, just at the limit of detectability ($\log K_{H_6L(F)/H_6L\cdot F} \approx 2$).[56] However, the divalent sulfate interacts relatively strongly with $\mathbf{L}^1$. Again, this finding was anticipated by documented general trends for binding in polyammonium systems, indicating that anion affinity tends to increase with increasing charge on the anion.[8-18]

It was expected that the binding constants for $\mathbf{L}^2$ would be about 1−2 orders of magnitude higher than those for $\mathbf{L}^1$. Again, a clear dependence on charge exists, with the affinity of $\mathbf{L}^2$ for sulfate an order of magnitude higher than that for nitrate. Fluoride binding with $\mathbf{L}^2$ was also found to be slightly higher than that observed for nitrate ($\log K_{H_6L(F)/H_6L\cdot F} = 3.56(3)$ and $\log K_{H_7L(F)/H_7L\cdot F} = 4.29(4)$).[56] As in the nitrate case, crystallographic[27,56] and ^{19}F NMR results[27] indicated encapsulated fluoride. Of special interest, however, are the relatively large binding constants observed for sulfate with both $\mathbf{L}^1$ and $\mathbf{L}^2$. In fact, the affinities of $\mathbf{L}^1$ for sulfate almost rival those observed for $\mathbf{L}^2$. Recent findings of a related neutral amide corollary of $\mathbf{L}^1$ also indicated selective binding of sulfate as well as phosphate over other monovalent anions, although in nonaqueous conditions. The overall structure and the pattern of hydrogen-bonding interactions are significantly different from those observed in $\mathbf{L}^1$, however.[59]

As a result of the crystallographic findings for the nitrate complex with $\mathbf{L}^2$, indicating two internal nitrates, we were especially interested in whether the binding of the bicycle $\mathbf{L}^2$ with nitrate could also be described using a binuclear model. In fact, our preliminary studies indicated that a binuclear model fit the data.[28] Unfortunately, it is difficult to draw definitive conclusions about the stoichiometry with only potentiometric measurements, because K_s was observed to drift with anion concentrations. Thus, repeated measurements under the experimental conditions of this study indicated that the best models are mononuclear 116 and 117 species as reported in Table 6.

It is true that a straightforward correlation between crystallographic results and studies performed in dilute solutions is handicapped by the interference of the many weak interactions found in solution. The species involved include the receptor, the anions, the electrolyte (including cations[60]), and in the case of water, a very noninnocent solvent highly capable of hydrogen-bonding and dipole interactions. Hydrogen bonding is also sensitive to concentration and especially pH. Nonetheless, it is our belief that while crystal structures may not be able to provide the entire story, they can provide significant information about solution chemistry. A case in point can be seen in the comparative study of fluoride binding with $\mathbf{L}^2$ using solution ^{19}F NMR techniques in conjunction with solid-state crystallographic findings (both of which indicate internally bound fluoride).[27]

The general conclusion of these binding studies is, however, that flexible monocycles, as exemplified by this type of Schiff base-derived receptors, are not viable candidates for generating highly selective receptor systems for anions. This conclusion agrees with that previously drawn from our earlier molecular dynamics studies.[1,9] On the other hand, the added dimensionality of the bicycle $\mathbf{L}^2$ appears to promote a higher affinity for a variety of anions. There is not any evidence, however, to indicate the existence of an exceptionally discriminating selectivity pattern for this particular azacryptand. This does not rule out the possibility for other azacryptands, as seen for example in the affinity patterns observed for a tiny octaazacryptand with fluoride[61-63] and more recently for chloride at pHs less than 2.5.[64]

Conclusions

Crystallographic findings lend considerable insight to the forces at play in these receptors. The macrocyclic systems all consist of elegant networks of hydrogen-bonding arrays in the crystalline state. $\mathbf{L}^1$ forms extensive hydrogen-bonding complexes with the both nitrate and sulfate, which hover above and below the macrocycle. The positioning of the anions in both complexes is quite similar and serves to mold the elliptical shape of $\mathbf{L}^1$ by bridging across the triamine chains. The structural information obtained on hydrogen-bonding interactions for the bicycle $\mathbf{L}^2$ proves that the well-demonstrated ditopic behavior of these systems for transition metal ions can be expanded to other types of species.[27,28,56] Furthermore, the overall structure of the cryptand is governed by multiple hydrogen-bonding interactions within and outside of the cavity, resulting in a variety of cavity sizes and shapes. In the tosylate structure, this means that the cavity is fairly open and accessible to other target anions. This finding supports the suppositions of early workers that the bulky tosylate and tosylate-related anions would not extensively interfere in anion binding studies.

(56) Aguilar, J. A.; Clifford, T.; Danby, A.; Llinares, J. M.; Mason, S.; García-España, E.; Bowman-James, K. *Supramol. Chem.*, in press.
(57) Menif, R.; Martell, A. E.; Squattrito, P. J.; Clearfield, A. *Inorg. Chem.* **1990**, *29*, 4723−4729.
(58) Basallote, M. G.; Duran, J.; Fernandez-Trujillo, M. J.; Mañez, M. A.; Szpoganicz, B. *J. Chem. Soc., Dalton Trans.* **1999**, 1093−1100.
(59) Hossain, M. D.; Llinares, J. M.; Powell, D.; Bowman-James, K. *Inorg. Chem.* **2001**, *40*, 2936−2937.
(60) Bencini, A.; Bianchi, A.; Giorgi, C.; Fusi, V.; Masotti, A.; Paoletti, P. *J. Org. Chem.* **2000**, *65*, 7686−7689.
(61) Dietrich, B.; Lehn, J.-M.; Guilhem, J.; Pascard, C. *Tetrahedron Lett.* **1989**, *30*, 4125−4128.
(62) Dietrich, B.; Dilworth, B.; Lehn, J.-M.; Souchez, J.-P.; Cesario, M.; Guilhem, J.; Pascard, C. *Helv. Chim. Acta* **1996**, *79*, 569−587.
(63) Reilly, S. D.; Khalsa, G. R. K.; Ford, D. K.; Brainard, J. R.; Hay, B. P.; Smith, P. H. *Inorg. Chem.* **1995**, *34*, 569−575.
(64) Hossain, M. D.; Llinares, J. M.; Miller, C. A.; Seib, L.; Bowman-James, K. *Chem. Commun.* **2000**, 2269−2270.

Binding studies indicate that the monocycle has little affinity for monanions, although significant binding was observed for divalent sulfate. Considering the structural results in conjunction with the potentiometric studies, there is no indication that the monocycle $\mathbf{L}^1$ shows promise for highly selective anion binding. Binding for both nitrate and sulfate was enhanced for the azacryptand $\mathbf{L}^2$. While the complementarity of $\mathbf{L}^2$ for nitrate is almost ideal on the basis of the crystal structure results, the azacryptand still shows higher selectivity for the divalent sulfate ion. Thus, while an increase in the dimensionality of these polyammonium receptors results in higher affinities, discrimination and selectivity based on factors other than just anion charge do not appear to have a major influence on the magnitude of anion binding.

Acknowledgment. This research was sponsored by the Environmental Management Science Program, Offices of Science and Environmental Management, U.S. Department of Energy under Grant DE-FG-96ER62307. The authors thank Larry Seib of the X-ray Crystallography Laboratory at the University of Kansas and Alicia Beatty at the X-ray Crystallography Laboratory at Kansas State University for assistance in structure determinations. The help of Martha Morton and David Vander Velde of the NMR Laboratory and Todd Williams of the Mass Spectrometry Laboratory at the University of Kansas is also appreciated. Cynthia Miller and Paula Sage in the K.B.-J. group are thanked for their assistance in some of the studies.

Supporting Information Available: Five crystallographic files in CIF format. This material is available free of charge via the Internet at http://pubs.acs.org.

IC010135L